

Article

Instrumental Photon Activation Analysis with Short-Time Irradiation for Geochemical Research

Ivana Krausová^{1,2}, Jiří Mizera^{1,3,*} , Zdeněk Řanda¹, David Chvátíl¹ and Pavel Krist¹

¹ Nuclear Physics Institute, Czech Academy of Sciences, 250 68 Řež, Czech Republic; krausova@ujf.cas.cz (I.K.); vera.randova@iex.cz (Z.Ř.); chvatil@ujf.cas.cz (D.C.); krist@ujf.cas.cz (P.K.)

² Faculty of Agrobiological Sciences, Food and Natural Resources, Czech University of Life Sciences Prague (CZU), Kamýcká 129, 165 00 Prague, Czech Republic

³ Institute of Rock Structure and Mechanics, Czech Academy of Sciences, V Holešovičkách 41, 182 09 Prague, Czech Republic

* Correspondence: mizera@ujf.cas.cz

Abstract: This paper introduces instrumental photon activation analysis (IPAA) utilizing short-lived products of photonuclear reactions, mainly (γ, n) and (γ, p) , initiated by bremsstrahlung from the MT-25 microtron. A rapid nondestructive IPAA method for geochemical major element analysis is introduced as a tool for the basic geochemical characterization of rocks. Procedures were developed and parameters such as beam energy and irradiation-decay-counting times optimized with a representative set of geochemical reference materials, and an optimized scheme was applied in analysis of various geological samples. A complete analytical scheme combined with long-time irradiation IPAA and the possibility of utilization of photoexcitation reactions (γ, γ') are briefly outlined.

Keywords: IPAA; geochemical analysis; whole-rock analysis; major elements; microtron



Citation: Krausová, I.; Mizera, J.; Řanda, Z.; Chvátíl, D.; Krist, P. Instrumental Photon Activation Analysis with Short-Time Irradiation for Geochemical Research. *Minerals* **2021**, *11*, 617. <https://doi.org/10.3390/min11060617>

Academic Editor: Pieter Bertier

Received: 5 May 2021

Accepted: 7 June 2021

Published: 9 June 2021

Publisher's Note: MDPI stays neutral with regard to jurisdictional claims in published maps and institutional affiliations.



Copyright: © 2021 by the authors. Licensee MDPI, Basel, Switzerland. This article is an open access article distributed under the terms and conditions of the Creative Commons Attribution (CC BY) license (<https://creativecommons.org/licenses/by/4.0/>).

1. Introduction

The basic geochemical characterization of rocks, minerals, sediments, soils, and other materials usually comprises determination of major elements Si, Al, Mn, Mg, Ca, Fe, Ti, Na, K, and P (as oxides) and other components released by thermal decomposition of the sample, such as CO₂ and moisture and essential (bound) water (H₂O⁻ and H₂O⁺, respectively). The analysis has also been applied in characterization of construction materials such as concrete, mortars, plasters, bricks, cinderblocks, etc. Classical whole or rapid rock analyses are destructive methods, requiring combustion or fusion and dissolution of the sample, and involve tedious procedures such as gravimetry, colorimetric, potentiometric, or coulometric titrations [1]. Even replacing the classical procedures with instrumental spectrometric techniques such as AAS, ICP-AES(OES), or ICP-MS [1,2] still requires sample dissolution. Not only does complete sample destruction prevent reanalyzing or further analyzing the sample, but it also presents a risk of loss of an analyte or its incomplete dissolution, particularly for some resistant minerals. That is why the arrival of nondestructive methods, namely various modes of activation analysis and X-ray fluorescence (XRF) analysis was quite revolutionary. In the case of the activation analysis, because it makes the sample radioactive and possibly modifies it by radiation effects, the non-destructiveness must be understood as stated above, i.e., preserving the sample for further analyses without impact on the future results and for its further use in an intended manner. On the other hand, despite the undisputable power and the present leading position of XRF for geochemical (mainly major element) analysis, in XRF one must consider and avoid or treat various inter-element interferences, the spectral background, sample matrix effects, incorrect sample preparation [3], and limitations of surface analysis for bulk, heterogeneous samples. Some of those problems have been overcome with dedicated mathematical corrections applied in the current instrumentation and by application of the fused bead technique. The latter, however, lacks the advantage of non-destructiveness.

Radioanalytical nuclear methods suitable for geochemical, both major and trace element, analysis are represented by various modes of activation analysis: neutron and photon activation analyses (NAA [4,5] and PAA [5–9], respectively), and neutron-induced prompt gamma activation analysis (PGAA [10,11]). The activation methods are usually considered as nondestructive (in the above-mentioned sense) methods in their instrumental modes (INAA and IPAA; in PGAA there is only a nondestructive mode). Due to sample activation, PGAA and IPAA are gentler than is INAA, although the major element assay can almost completely be realized using a short-time irradiation mode of INAA, in which the sample is much less activated and production of long-lived radionuclides is strongly suppressed. Among the activation methods, INAA may have the greatest potential, but the major element determination for geochemical analysis in the short-time irradiation mode has some limitations. Determination of Si via ^{28}Al produced in the (n, p) reaction with fast neutrons requires selective activation with thermal neutrons being shielded (usually by irradiation in a Cd box). Determination of Fe usually requires longer irradiation due to the relatively long half-life of the activation product ^{59}Fe . Determination of P is limited by the inability to detect the produced pure beta-emitter ^{32}P by gamma-spectrometry; measuring its beta radiation usually requires radiochemical separation. Determination of Mg is hindered by several nuclear interferences, mainly the (n, p) reaction on Al whose correction significantly increases uncertainty in samples with higher Al contents [4,5].

In geochemical analysis, IPAA (known also as gamma activation analysis, mainly in older and Russian literature) represents an advantageous alternative to INAA [5–9]. A lower sensitivity of IPAA due to lower activation cross-sections and limited fluence rates in available irradiation facilities compared to that for INAA results in lower activities produced, and it allows for the analysis of larger and more representative samples (see Section 3.2). The more common long-time irradiation mode of IPAA usually allows nondestructive determination in rock and rock-based samples of the major elements Na, Mg, Ca, Ti, and Mn. The remaining elements Si, Al, K, Fe, and possibly P can be determined using the short-time irradiation IPAA based on short-lived (with half-lives of seconds to minutes) photoactivation products of (γ , n) and (γ , p) reactions, which are listed together with several other elements in Table 1. Most of the short-lived photoactivation products (^{23}Mg , ^{29}Al for Si, ^{48}Ti , ^{47}K for Ca, ^{53}Fe , ^{38}K) emit specific gamma lines, except for $^{26\text{m}}\text{Al}$ and ^{30}P , which are pure positron emitters. The latter ones can be detected only via the non-specific 511 keV annihilation line and are thus interfered with by other positron emitters. It is necessary to optimize the beam energy according to the reaction threshold and maximum energy (E_{thr} and E_{max} , respectively) and the decay and counting times for minimizing the effect of the interfering nuclides, i.e., other positron emitters, particularly ^{13}N and ^{15}O . Determination of P is limited due to quite similar half-lives and E_{thr} or E_{max} values of ^{30}P and ^{15}O (cf. Table 1). Measuring the non-annihilated positron radiation of ^{30}P using, e.g., a scintillation counter, would be a possible solution [12].

Table 1. Radionuclides and photonuclear reactions considered in application of the short-time irradiation for geochemical analysis [13,14].

Element	Photonuclear Reaction	Half-Life	Analytical Photopeak E_{γ} (keV)	E_{thr} (MeV) ^a	E_{peak} (MeV) _b	σ_{max} (mb) ^c	Target Natural Abundance (%)
C	$^{12}\text{C}(\gamma, n) ^{11}\text{C}$	20.4 min	511	18.7	23.4	8.7	98.9
N	$^{14}\text{N}(\gamma, n) ^{13}\text{N}$	9.97 min	511	10.6	23.3	14.7	99.6
O	$^{16}\text{O}(\gamma, n) ^{15}\text{O}$	2.04 min	511	15.7	17.2	2.9	99.8
Mg	$^{24}\text{Mg}(\gamma, n) ^{23}\text{Mg}$	11.3 s	439; 511	16.5	19.2	9.9	78.6
Mg	$^{26}\text{Mg}(\gamma, p) ^{25}\text{Na}$	59.6 s	974.2	14.1	17.8	5.1	11.0
Al	$^{27}\text{Al}(\gamma, n) ^{26\text{m}}\text{Al}$	6.35 s	511	13.3	21.2	15.8	100
Si	$^{29}\text{Si}(\gamma, p) ^{28}\text{Al}$	2.24 min	1778.8	12.3	~21	~20	4.7
Si	$^{30}\text{Si}(\gamma, p) ^{29}\text{Al}$	6.56 min	1273.4	13.5	n.a. ^d	n.a. ^d	3.1

Table 1. Cont.

Element	Photonuclear Reaction	Half-Life	Analytical Photopeak E_γ (keV)	E_{thr} (MeV) ^a	E_{peak} (MeV) _b	σ_{max} (mb) ^c	Target Natural Abundance (%)
P	$^{31}\text{P}(\gamma, n)^{30}\text{P}$	2.5 min	511	12.3	19.5	19	100
K	$^{39}\text{K}(\gamma, n)^{38}\text{K}$	7.61 min	2167.7	13.1	20	16	93.2
Ca	$^{48}\text{Ca}(\gamma, p)^{47}\text{K}$	17.5 s	2013	15.2	19.2	9.5	0.19
Fe	$^{54}\text{Fe}(\gamma, n)^{53}\text{Fe}$	8.51 min	377.9; 511	13.6	17.9	67	5.8
Zr	$^{90}\text{Zr}(\gamma, n)^{89m}\text{Zr}$	4.16 min	587.7; 511	12.6	16.4	159	51.5
Ba	$^{138}\text{Ba}(\gamma, n)^{137m}\text{Ba}$	2.55 min	661.7	9.2	15.3	354	71.7

^a Threshold energy. ^b Peak energy (at the first cross section maximum, if more peaks are present). ^c Peak cross section (1 mb = 10^{-31} m²).

^d Not available.

The rapid and economic short-time irradiation IPAA mode was tested in the 1970s in the Czech Republic [15], but the betatron accelerator employed then for irradiations provided an insufficient current of accelerated electrons (i.e., low photon fluence rates of produced bremsstrahlung); in addition, the absence of a system for fast sample transport precluded a wider application of the method. The present work demonstrates possibilities of the method under irradiation conditions provided by the MT-25 microtron accelerator of the Nuclear Physics Institute, Czech Academy of Sciences, with a recently installed automated pneumatic tube delivery system for rapid sample transport between the beam position and detector (Figures 1–3) [16,17].

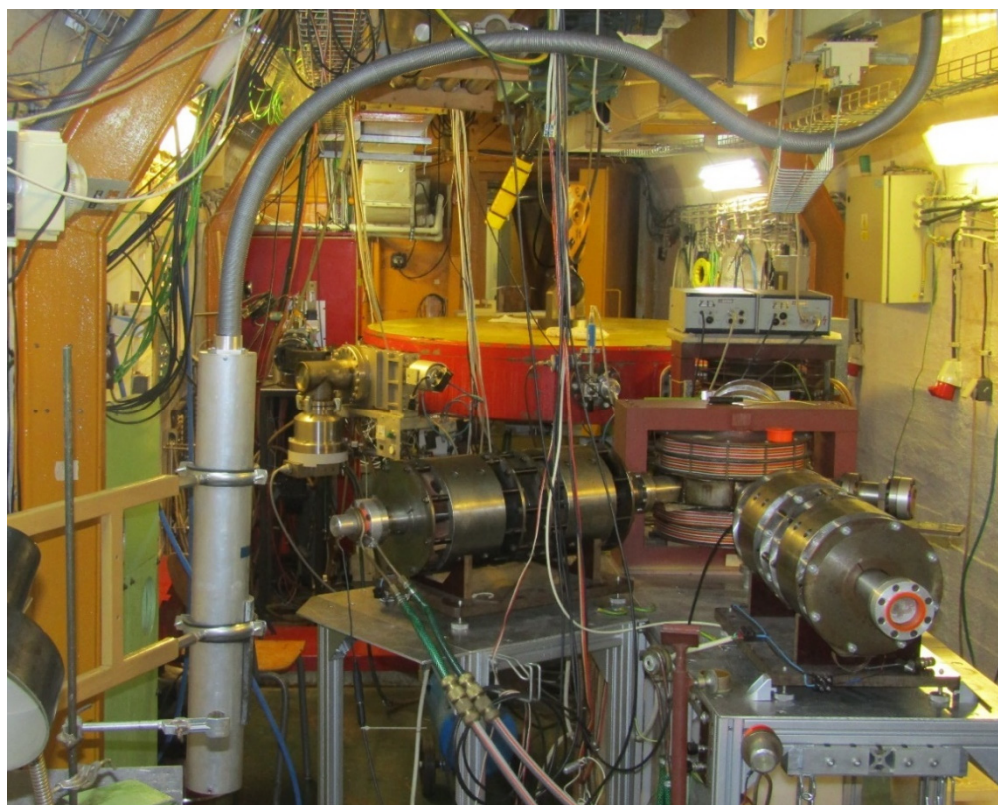


Figure 1. Microtron MT-25 with two electron beam outlets; the left one has the tungsten, water-cooled converter installed, and the irradiation terminal for short-time irradiations in the working position, connected to the main transporting tube of the pneumatic tube delivery system.



Figure 2. Components of the pneumatic tube delivery system installed at the MT-25 microtron. **Left:** 4-way routing head installed above the detector shielding with positions for sample insertion and delivery to the irradiation terminal (and back), counting position, and discarding position. **Right:** Sample in irradiation vial at the counting position on the detector inside the shielding.

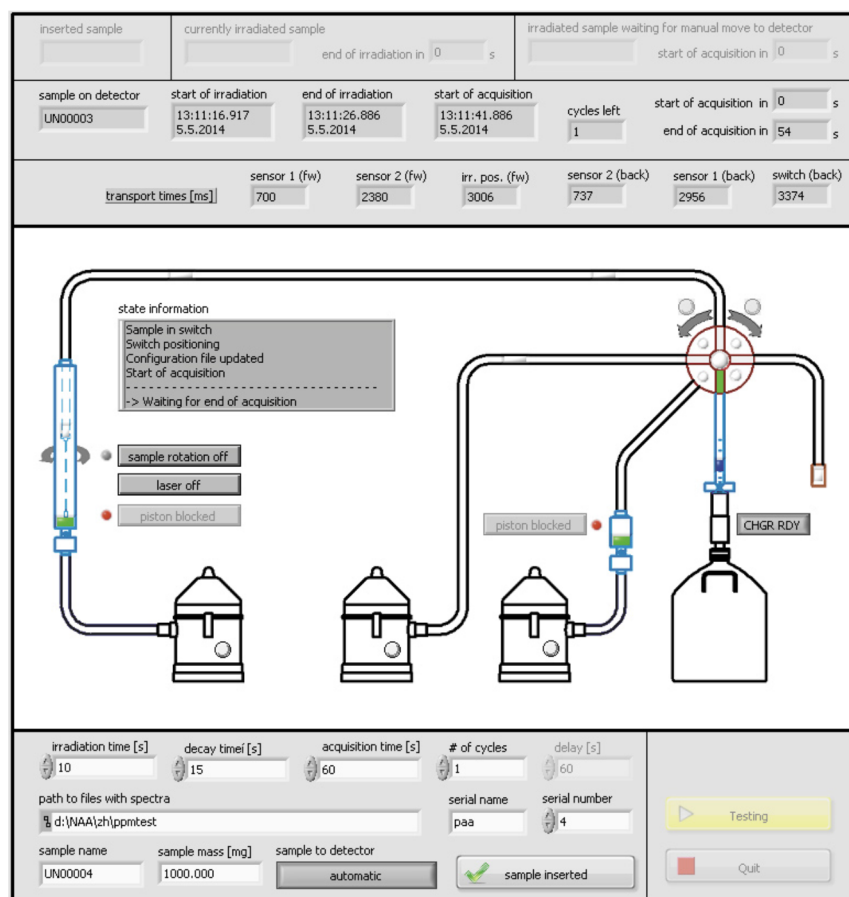


Figure 3. Graphical user interface for the control of the pneumatic tube delivery system showing its schematic design (from left to right: irradiation terminal, 3 vacuum cleaners, 4-way routing head, detector with a Dewar cooling). Reproduced from [17] with permission from Springer Nature.

2. Materials and Methods

2.1. Sample Preparation and Calibration Standards

Geological reference materials and rock samples were weighed (100 to 2500 mg depending on availability) directly into transport-counting vials (25 mL, HDPE). The reference materials selected to represent various rock types included serpentine CNRS UB-N, granite CNRS GS-N, basalt CNRS BE-N, andesite USGS AGV-2, quartz latite USGS QLO-1, and trachyte CNRS ISH-G. The rock samples included samples previously analyzed in our laboratory by INAA: Central European tektites—moldavites—MM 56 (Rouchovany, Moravia, Czech Republic), SBM 184 (Pištín, south Bohemia, Czech Republic), and phonolite NBPH3 (Sokol Hill in the Lusatian Mts., north Bohemia, Czech Republic). Multi-element calibration standards of Si, Fe, K, Zr, Ba, and Sr and single-element standards of Mg and Al were prepared from suitable stoichiometric, well characterized compounds by weighing (50–800 mg) and mixing with starch (all analytical grade reagents) to achieve identical geometry of standards and samples (for details, see [16]).

2.2. Irradiation at MT-25 and Gamma-Spectrometric Measurement

The high energy photon radiation used in PAA can be obtained in a microtron—a radio frequency cyclic accelerator of electrons—as the bremsstrahlung, produced by braking of the accelerated electron beam on a heavy (e.g., tungsten) target—converter. The microtron MT-25 employed in the present paper is shown in Figure 1 and its basic parameters are briefly described in, e.g., [17]. Fast, online (i.e., without switching off the accelerator) irradiation-counting cycles are enabled by a pneumatic tube delivery system. The system (see Figures 1–3) allows for the transport of an irradiated sample between the irradiation position and detector (about 30 m) and for counting 6 s after the end of the irradiation. In the offline mode that requires switching off the accelerator, ventilating the space to reduce produced ozone, opening the shielding doors, and carrying the sample to the detector, at least 3 min are required, leading to an increased radiation burden of personnel. Fluctuation of the current of accelerated electrons requires measurement and recording for use in normalizing the results [16,17].

Gamma spectra of both standards and samples were acquired using a coaxial HPGe detector (Intertechnique, Strasbourg, France), with a relative efficiency of 21% and FWHM of 1.85 keV for 1332.5 keV photons of ^{60}Co , connected to a LynxTM DSP gamma-spectrometric system controlled by the Genie 2000 v. 3.3 software (Canberra, Meriden, CT, USA). Identical counting geometry (about 1 cm from the detector top) was used for all spectra acquisitions.

Determination of elemental contents is based on determining the pure area (without background) of an analytical photopeak $P(t_i, t_d, t_c)$ of a photoactivation product, defined as ([8], modified):

$$P(t_i, t_d, t_c) = \frac{mSDCt_c}{A_r} N_A \theta \eta h \int_{E_{thr}}^{E_{max}} \phi(E) \sigma(E) dE \quad (1)$$

Here, t_i , t_d , t_c are the irradiation, decay, and counting times, respectively, m is the mass of the element in the target (sample or standard), θ is the natural isotopic abundance of the analytical isotope of the element, η is the detector efficiency at a given peak energy, h is the emission probability of the photopeak, A_r is the relative atomic mass of the element, N_A is the Avogadro constant, E_{thr} is the threshold energy, $\sigma(E)$ is the cross section of the production photonuclear reaction, E_{max} is the maximum energy, $\phi(E)$ is the photon flux density of the applied photon radiation (bremsstrahlung), and S , D , C are the saturation, decay, and counting factors, respectively, defined as:

$$S = 1 - e^{-\lambda t_i} \quad (2)$$

$$D = e^{-\lambda t_d} \quad (3)$$

$$C = (1 - e^{-\lambda t_c}) / \lambda t_c \quad (4)$$

Here, λ is the decay constant of the photoactivation product.

Element concentrations (mass fractions), however, were not calculated directly using Equation (1). Instead, a direct comparator method was used, which is based on comparison of the analytical photopeak areas of the analyzed sample (unknown) and a comparator (calibrator, standard) with known element concentration, according to an equation derived from Equation (1):

$$C_{un} = C_{st} \frac{P_{un} (wSDCQt_c)_{st}}{P_{st} (wSDCQt_c)_{un}} \quad (5)$$

Here, the indices *un* and *st* denote unknown and standard, respectively, and *w* is a weight of the analyzed sample or standard aliquot. The parameter *Q* is the charge calculated from the accelerated electron current recorded during irradiation and it is a proxy for the photon flux in Equation (1) used for normalizing the photopeak areas to an equal photon dose. The remaining quantities are the same as those defined above.

The choice of optimum irradiation conditions has been based on the normalized reaction rate R_n for an individual element (its photoactivation product), which represents its saturation activity (in Bq) obtained after irradiating a target containing 1 g of a pure element using a 1 μ A beam of accelerated electrons:

$$R_n = \frac{Pt_i}{mSDCt_c\theta\eta hQ} \quad (6)$$

All symbols in the equation have already been defined with the equations above.

3. Results and Discussion

3.1. Reaction Rates

In order to optimize the beam energy, the calibration standards were irradiated at the beam energies 17, 18, 19, and 21 MeV, varying also the irradiation-decay-counting times ($t_i-t_d-t_c$). The $t_i-t_d-t_c$ regimes 600-6-600 s, 600-6-900 s, 600-180-600 s, 600-300-600 s, and 600-300-900 s were tested with the multi-element calibration standards. The shortest-lived products of Mg and Al irradiation were tested with their standards using the time regimes 10-6-10 s, 40-6-40 s, 50-6-50 s, and 60-6-60 s. The normalized reaction rates R_n were calculated using Equation (6); selection of the R_n values for optimal time regimes are presented in Table 2. Due to high photoactivation cross sections, radionuclides ^{89m}Zr and ^{137m}Ba (see Table 1) were produced in detectable activities and thus included as “by-products” in the IPAA determination of major elements. The radionuclide ^{47}K , quite a short-lived product of Ca photoactivation (see Table 1), was not detected in most tests, even considering the sensitive Ca determination by IPAA with long-time irradiation (see below); therefore, it was not further tested. The R_n values in Table 2 indicate that for all major elements, higher beam energies of 19 and 21 MeV are favorable. The determination of trace elements of Ba and Zr is much more sensitive and was slightly more favorable at a lower beam energy of 18 MeV, in agreement with higher cross sections and lower threshold energies of their production reactions (see Table 1).

Table 2. Variation of the normalized reaction rate R_n ($\text{Bq g}^{-1} \mu\text{A}^{-1}$) of the analytical photoactivation products with the beam energy.

Beam Energy	^{53}Fe ^a	^{38}K ^a	$\text{Si}(^{29}\text{Al})$ ^a	^{137m}Ba ^a	^{89m}Zr ^a	^{23}Mg ^b	^{26m}Al ^c
17 MeV	1.4×10^3	1.3×10^4	n.d. ^d	2.5×10^5	2.7×10^5	n.d. ^d	n.d. ^d
18 MeV	9.7×10^3	6.9×10^4	1×10^3	6.7×10^5	1.1×10^6	-	-
19 MeV	1.1×10^4	8.7×10^4	3×10^3	2.7×10^5	7.9×10^5	2.1×10^4	1.5×10^5
21 MeV	1.3×10^4	1.1×10^5	2×10^3	4.7×10^5	9.3×10^5	1.2×10^5	1.4×10^5

^a $t_i-t_d-t_c$ 600-180-600 s. ^b $t_i-t_d-t_c$ 40-60-40 s. ^c $t_i-t_d-t_c$ 10-6-10 s. ^d Not detected.

3.2. Determination of Si, Fe, K, Ba, and Zr

Validation of the IPAA procedure for Si, Fe, K, Ba, and Zr determination was carried out in the $t_i-t_d-t_c$ regime 600-180-600 s at various beam energies. Results are presented in Table 3. In agreement with the previous optimization based on evaluation of the normalized reaction rate R_n , the optimum beam energy was 19 MeV for Si, Fe, and K determination and 18 MeV for Ba and Zr determination. With these beam energies, the best match of the contents determined by IPAA with certified values was obtained. Because Ba and Zr are just “by-products” in the determination of major elements, 19 MeV was chosen as the optimum beam energy for further analyses of the rock samples. In Figure 4, a typical gamma spectrum obtained in this part of IPAA with short-time irradiation is shown in comparison with a spectrum obtained in INAA with short-time irradiation. In IPAA compared to INAA, note the different radionuclides produced (β^+ vs. β^- emitters, respectively, reflected by a more pronounced annihilation line 511 keV in IPAA) in addition to much lower activities induced (regarding the analyzed sample masses and counting geometries) and higher peak-to-background ratios.

Table 3. Contents of Si, Fe, and K (recalculated to oxides, wt.% \pm U^a) and Ba and Zr ($\mu\text{g}\cdot\text{g}^{-1}$) determined by IPAA in geological reference materials at various beam energies, with a $t_i-t_d-t_c$ regime of 600-180-600 s.

		17 MeV	18 MeV	19 MeV	21 MeV	Certified Value ^b
SiO ₂	CNRS UB-N	Not activated	40.4 \pm 1.50	41.30 \pm 1.79	37.96 \pm 0.97	39.43 \pm 0.15
	CNRS GS-N	Not activated	68.08 \pm 2.44	65.96 \pm 2.64	65.50 \pm 1.62	65.80 \pm 0.19
	CNRS BE-N	Not activated	43.72 \pm 1.75	39.12 \pm 1.62	35.02 \pm 1.05	38.20 \pm 0.12
	USGS QLO-1	Not activated	70.09 \pm 2.62	66.30 \pm 2.83	54.61 \pm 1.37	65.6 \pm 0.47
	USGS AGV-2	Not activated	65.84 \pm 1.23	58.46 \pm 3.02	Not analyzed	59.3 \pm 0.70
Fe ₂ O ₃	CNRS UB-N	9.88 \pm 0.55	8.21 \pm 0.20	8.60 \pm 0.25	8.01 \pm 0.20	8.34 \pm 0.1
	CNRS GS-N	4.35 \pm 0.59	3.71 \pm 0.12	3.86 \pm 0.14	3.54 \pm 0.15	3.75 \pm 0.04
	CNRS BE-N	15.84 \pm 0.88	14.53 \pm 0.33	13.07 \pm 0.31	10.55 \pm 0.15	12.84 \pm 0.06
	USGS QLO-1	4.60 \pm 0.41	4.65 \pm 0.13	4.61 \pm 0.15	3.70 \pm 0.13	4.35 \pm 0.14
	USGS AGV-2	7.27 \pm 0.49	7.10 \pm 0.17	6.36 \pm 0.15	Not analyzed	6.69 \pm 0.13
K ₂ O	CNRS UB-N	<0.03	<0.01	0.015 \pm 0.001	0.019 \pm 0.002	0.02 \pm 0.001
	CNRS GS-N	5.23 \pm 0.18	4.65 \pm 0.10	4.68 \pm 0.10	4.70 \pm 0.10	4.53 \pm 0.06
	CNRS BE-N	1.62 \pm 0.07	1.50 \pm 0.02	1.40 \pm 0.07	1.36 \pm 0.03	1.39 \pm 0.02
	USGS QLO-1	3.86 \pm 0.12	3.57 \pm 0.03	3.69 \pm 0.08	3.58 \pm 0.07	3.60 \pm 0.12
	USGS AGV-2	3.11 \pm 0.10	2.87 \pm 0.06	2.98 \pm 0.06	Not analyzed	2.88 \pm 0.11
Ba	CNRS UB-N	<19.8	21.2 \pm 4.2	<18.9	<26.1	27 \pm 3
	CNRS GS-N	1655.1 \pm 33.1	1432.9 \pm 28.7	1460.5 \pm 29.2	1552.8 \pm 31.1	1400 \pm 44
	CNRS BE-N	1303.5 \pm 26.1	1270.6 \pm 25.4	1082.9 \pm 21.6	1117.6 \pm 22.4	1025 \pm 30
	USGS QLO-1	1338.8 \pm 26.8	1424.2 \pm 28.5	1517.9 \pm 30.4	1366.8 \pm 27.4	1370 \pm 80
	USGS AGV-2	1208.6 \pm 24.2	1162.4 \pm 23.2	1268.3 \pm 25.3	Not analyzed	1140 \pm 32
Zr	CNRS UB-N	<8.6	<3.8	<5.8	<9.1	4 \pm 1
	CNRS GS-N	297 \pm 15	249 \pm 12	262 \pm 7	261 \pm 8	235 \pm 8
	CNRS BE-N	312 \pm 11	315 \pm 14	306 \pm 8	222 \pm 7	260 \pm 5
	USGS QLO-1	170 \pm 9	183 \pm 10	204 \pm 6	176 \pm 6	185 \pm 8
	USGS AGV-2	272 \pm 9	239 \pm 5	252 \pm 7	Not analyzed	230 \pm 2

^a Combined standard uncertainty contributed mainly by counting statistics and fluctuation in irradiation-counting geometries (root sum of squares of individual type B uncertainty estimates, 1). ^b Standard deviation according to the certificate specification. The bold indicates the “best” results (optimum energy).

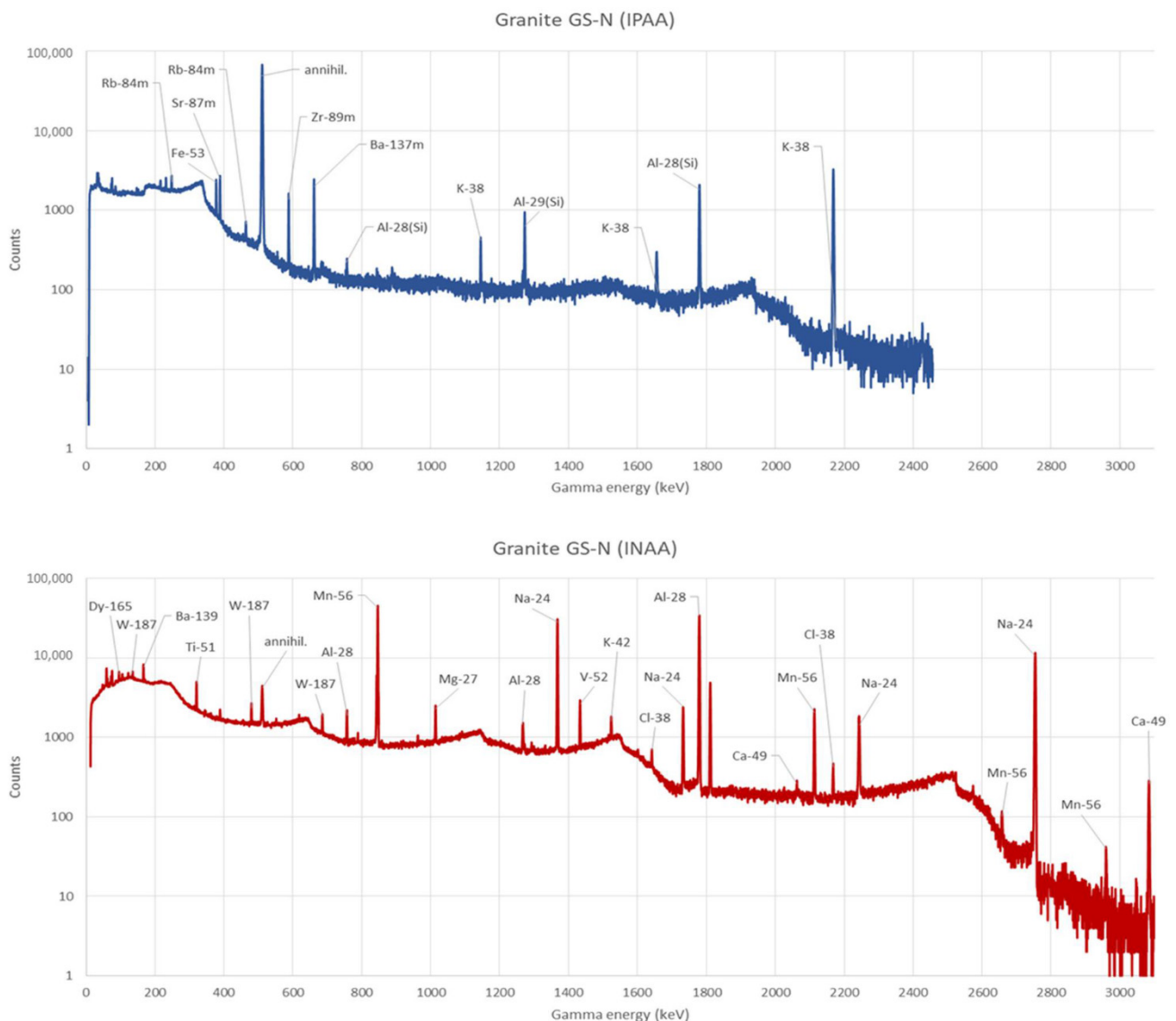


Figure 4. A typical gamma spectrum obtained in IPAA with short-time irradiation (blue spectrum) in comparison with a spectrum obtained in INAA with short-time irradiation (red spectrum) for the analysis of granite CNRS GS-N. IPAA: 2.5 g sample, irradiation at the MT-25 microtron, 19 MeV beam energy, $t_i-t_d-t_c$ 600-180-600 s, counting 1 cm from detector top (see Section 3.2 and Table 3). INAA: 0.05 g sample, irradiation at the LVR-15 reactor of the Research Center Řež, $t_i-t_d-t_c$ 1-13-13 min, counting 15 cm from detector top.

Results of Si, Fe, K, Ba, and Zr determination in samples of moldavites and a phonolite are presented in Table 4. For quality control, trachyte CNRS ISH-G was used. Acceptable agreement was achieved with reference values, and also with results from previous analyses of the samples by INAA and IPAA with long-time irradiation, for which, however, uncertainties were not available.

Table 4. Contents of Si, Fe, and K (recalculated to oxides, wt.% \pm U^a) and Ba and Zr ($\mu\text{g g}^{-1}$) determined by IPAA in a phonolite and two moldavite samples, with CNRS ISH-G trachyte used for quality control. Beam energy 19 MeV, t_i - t_d - t_c regime 600-180-600 s.

Sample	SiO ₂	Fe ₂ O ₃	K ₂ O	Ba	Zr
NBPH3 ^b	56.55 \pm 2.47 (not analyzed)	2.61 \pm 0.12 (2.39 \pm 0.1)	4.72 \pm 0.10 (4.45 \pm 0.65)	<24.7 (126 \pm 56)	2860 \pm 56 (2910 \pm 58)
MM 56 ^b	84.78 \pm 4.40 (85.6)	1.92 \pm 0.16 (FeO) (1.71)	3.78 \pm 0.08 (3.57)	897 \pm 43 (797)	242 \pm 9 (275)
SBM 184 ^b	80.45 \pm 4.15 (79.0)	1.48 \pm 0.12 (FeO) (1.29)	3.24 \pm 0.07 (3.02)	819 \pm 41 (687)	266 \pm 7 (238)
CNRS ISH-G ^c	64.14 \pm 2.58 (58)	4.94 \pm 0.16 (4.9)	6.73 \pm 0.15 (6.49)	725 \pm 42 (660)	418 \pm 10 (370)

^a Combined standard uncertainty (see Table 3 for definition). ^b NBPH3—phonolite (Sokol Hill, Lusatian Mts., north Bohemia), MM 56—moldavite (Rouchovany, Moravia), SBM 184—moldavite (Pištín, south Bohemia). Reference values determined previously in our laboratory by INAA and IPAA with long-time irradiation (Zr) given in parenthesis. ^c Working values from the certificate given in parenthesis.

3.3. Determination of Al and Mg

Validation results for determining Mg and Al in the reference materials are presented in Table 5. Because ^{26m}Al can be measured only via the nonspecific annihilation gamma line 511 keV, a significant interference from other positronic emitters cannot be excluded despite a very short irradiation time ($t_i = 10$ s). For Al determination, a single t_i - t_d - t_c regime 10-6-10 s was applied. At a 17 MeV beam energy, ^{26m}Al was not sufficiently produced, i.e., the 511 keV peak was not detected. At both 19 and 21 MeV, the 511 keV peak was detected with acceptable counting statistics (uncertainty). Only the 511 keV peak was identified in spectra. Calculation of Al content assumed that the pure peak area belongs to ^{26m}Al only. Better agreement with certified values was obtained at 19 MeV. At 21 MeV, IPAA provided higher Al content in the USGS QLO-1 and USGS AGV-2 reference materials, possibly indicating an unknown interference. From the short-lived photoactivation products listed in Table 1, ²³Mg with a half-life similar to that of ^{26m}Al, and despite a higher threshold with a lower peak energy, is the most probable interfering nuclide at 21 MeV beam energy, regardless of the absence of its specific gamma line in the measured spectra. Interferences from ³⁰P and ¹⁵O are also possible, the former due to a low threshold energy and the latter due to generally high oxygen contents in rock samples. For distinguishing and subtraction of the interferences, time analysis of the 511 keV peak requiring continuous (differential instead of integral) activity measurement would be necessary.

Table 5. Contents of Al and Mg (recalculated to oxides, wt.% \pm U^a) determined by IPAA in geological reference materials at 19 MeV and 21 MeV beam energies and t_i - t_d - t_c regimes 10-6-10 s (Al) and 40-6-40 s (Mg).

		19 MeV	21 MeV	Certified Value ^b
Al ₂ O ₃	CNRS GS-N	14.83 \pm 0.35	14.80 \pm 0.35	14.67 \pm 0.09
	USGS QLO-1	17.10 \pm 0.53	18.70 \pm 0.44	16.2 \pm 0.19
	USGS AGV-2	17.18 \pm 0.40	22.53 \pm 0.53	16.91 \pm 0.21
MgO	CNRS UB-N	31.0 \pm 3.2	37.4 \pm 2.7	35.21 \pm 0.14
	CNRS GS-N	<2.83	<1.53	2.20 \pm 0.05
	CNRS BE-N	15.13 \pm 1.87	10.89 \pm 1.08	13.15 \pm 0.08
	USGS QLO-1	<0.45	<2.07	1.0 \pm 0.07

^a Combined standard uncertainty (see Table 3 for definition). ^b Standard deviation according to the certificate specification. The bold indicates the “best” results (optimum energy).

As for Mg, production of ²³Mg should be negligible at 17 and 18 MeV due to barely exceeding the threshold energy (cf. Table 1), thus similarly to Al, only higher beam energies 19 and 21 MeV were tested. Due to a relatively low cross section of the reaction ²⁴Mg(γ , n)²³Mg, Mg was below a limit of detection in CNRS GS-N and USGS QLO-1 reference

materials. Determination via the reaction $^{26}\text{Mg}(\gamma, p)^{25}\text{Na}$ proved to be even less sensitive. Extending t_i and t_c had no positive effect. Obviously, determination of Mg via its short-lived photoactivation products has much worse analytical potential than does determination via its longer-lived product ^{24}Na .

3.4. Complete Combined IPAA Procedure for Geochemical Major Element Analysis

Table 6 summarizes a complete combined IPAA procedure for the geochemical major element analysis consisting of two or three stages with different t_i - t_d - t_c time regimes and beam energies. All three stages could be realized with a single sample aliquot after sufficient decay times (ten minutes and one hour between the stages 1–2 and 2–3, respectively). In stage 1, only Al determination is possible with the t_i - t_d - t_c regime 10-6-10 s. Determination of Mg, Ca, and Ti would require additional irradiation and counting with a different t_i - t_d - t_c regime (40-6-40 s), but due to lower sensitivity it is more advantageous to determine these elements in the “long-time” of stage 3. In stage 2, P could be determined by counting β^+ radiation of ^{30}P using a scintillation detector. That, however, would require additional irradiation not only with a different t_i - t_d - t_c regime but also at a lower beam energy to minimize interferences (300-60-200 s and 17 MeV used in [12]). Stage 3 is in fact identical with a regular IPAA with long-time irradiation, which provides determination of major elements and determination of a number of minor and trace elements, including Na, Mg, Cl, Ca, Sc, Ti, Cr, Mn, Fe, Co, Ni, Cu, Zn, As, Br, Rb, Sr, Y, Zr, Nb, Mo, Ag, Cd, Sn, Sb, I, Cs, Ba, Ce, Nd, Sm, Au, Tl, Pb, Th, and U, which may be reduced depending on the type of rock analyzed [5]. In the long-time irradiation mode, it is possible and desirable to simultaneously irradiate a whole suite of samples, the size of which depends on available irradiation geometry and counting possibilities (e.g., beam current and geometry, number and space of irradiation positions, and number and efficiency of available detectors). It may be desirable to reduce sample size, which is also possible by taking aliquots from samples already analyzed in stages 1 and 2 and decayed for several hours.

Table 6. Summary of a complete combined IPAA procedure for geochemical major element analysis.

Stage	Elements (Photoactivation Products; Half-Life)	t_i - t_d - t_c	Beam Energy
1 (short-time)	Al (^{26}mAl ; 6.4 s) ^a	10-6-10 s 40-6-40 s ^b	18–19 MeV 19–21 MeV
	Mg (^{23}Mg ; 11.3 s) ^{a,b}		
	Mg (^{25}Na ; 59.6 s) ^b		
	Ca (^{47}K ; 17.5 s) ^b		
	Ti (^{46}mSc ; 18.7 s) ^b		
2 (medium-time)	Si (^{29}Al ; 6.6 min)	600-180-600 s	19–21 MeV
	Si (^{28}Al ; 2.24 min)		
	Fe (^{53}Fe ; 8.5 min)		
	K (^{38}K ; 7.6 min)		
	Ba (^{137}mBa ; 2.55 min)		
	Zr (^{89}mZr ; 4.16 min)		
	P (^{30}P ; 2.2 min) ^c		
3 (long-time)	Ca (^{43}K ; 22.3 h)	$t_i \approx 5$ –6 h $t_d \approx 1$ –20 d ^d $t_c \approx \text{min to h}$ ^d	22 MeV
	Mg (^{24}Na ; 14.7 h)		
	Mn (^{54}Mn ; 312.2 d)		
	Ti (^{47}Sc ; 3.3 d), Ti (^{48}Sc ; 1.8 d)		
	Na (^{22}Na ; 2.6 y)		

^a Analysis of the 511 keV line. ^b Additional irradiation-counting necessary. ^c Additional irradiation and positron counting; beam energy and time regime from [12]. ^d According to elements to be determined, up to 4 counting cycles applied, with t_c extended in later counting stages.

The requirement to perform the geochemical major element analysis by IPAA in several stages may handicap it in comparison with INAA. However, INAA does not provide in its short-time irradiation mode a complete analysis. In INAA, an additional irradiation

in a Cd shielding is necessary for Si determination, Fe and often also K determination needs long-time irradiation to reach a sufficient sensitivity, and P determination also requires a separate detection of beta radiation and also radiochemical separation. The problematic determination of Mg strongly interfered with by Al should also be considered. On the other hand, a great potential of IPAA for analysis of larger (and thus more representative) samples than are possible with INAA should be considered.

4. Potential of Short-Lived Photoexcitation Products

In the short-time irradiation mode of IPAA, a potential of the photoexcitation reactions (γ, γ') for geochemical analysis should be considered [6,9,15,18]. These reactions, which can be considered as inelastic photon scattering, have low threshold energies (mostly < 1 MeV) and on medium Z to heavy nuclei (Se and heavier) produce several isomeric radionuclides with half-lives of several seconds to several hours (see Table 7). The isomers mostly de-excite through emission of one or two photons. Yields of these reactions are quite low, with reaction cross sections in the μb range, and increase with an increase in the incident photon energy and reach maxima at about 10 MeV. On the other hand, the high selectivity of these reactions and counting with few interferences thanks to the absence of photodisintegration products below 7 MeV and good separation of analytical gamma lines are favorable.

Table 7. Main short-lived products of photoexcitation reactions (γ, γ') [15].

Element	Isomer	Half-Life	Analytical Photopeak E_γ (keV)	E_{thr} (MeV) ^a	Target Natural Abundance (%)
Se	^{77m} Se	17.4 s	161.9	0.17	7.6
Br	^{79m} Br	4.9 s	207.2	0.21	50.7
Sr	^{87m} Sr	2.80 h	388.4	0.39	7.0
Y	^{89m} Y	16.1 s	909.1	0.91	100
Rh	^{103m} Rh	56.1 min	39.75	0.04	100
Ag	^{107m} Ag	44.3 s	93.1	0.095	51.5
Ag	^{109m} Ag	39.8 s	88.0	0.09	48.7
Cd	^{111m} Cd	48.6 min	150.6; 245.4	0.40	12.8
In	^{113m} In	99.5 min	391.7	0.39	4.2
Ba	^{137m} Ba	2.55 min	660.6	0.662	11.3
Er	^{167m} Er	2.28 s	207.8	0.21	22.9
Yb	^{176m} Yb	11.8 s	292.9; 389.7	1.05	12.7
Lu	^{176m} Lu	3.68 h	88.4	0.30	2.6
Hf	^{179m} Hf	18.7 s	160.7; 215.5	0.38	13.8
W	^{183m} W	5.3 s	107.93; 160.5	0.31	14.4
Ir	^{191m} Ir	4.9 s	129.4	0.17	37.3
Au	^{197m} Au	7.8 s	278.5	0.41	100
Hg	^{199m} Hg	42.6 min	158.4; 374.1	0.53	16.8

^a Threshold energy.

As can be noticed in Table 7, some of the analytical gamma-rays of the photoexcitation products have rather low energies. Therefore, self-attenuation of gamma rays becomes much more pronounced than in the photonuclear reactions employed in the major element analysis, especially when analyzing larger samples with variable composition and using calibration standards with different densities (due to matrix compositions or grain size differences in samples). Necessary corrections have to be applied [19]. There may also be a limitation in materials with higher U and Th contents due to their photofission with the threshold energy of about 5.5 MeV. The natural activity and bremsstrahlung from the β^- emitters produced in the photofission increase the background in the spectra and thus also increase the detection limits for assayed elements.

A typical example of employing the short-time irradiation mode of IPAA with photoexcitation reactions is the rapid determination of gold in ore samples. More than one thousand large mass (hundreds of grams) samples collected during exploration of Au ores in several localities in the Czech Republic were analyzed in the 1980s using MT-22 microtrons (MT-25 predecessors, installed at the Czech Technical University in Prague and at the defunct Institute of Mineral Raw Materials in Kutná Hora) [18].

5. Conclusions

We demonstrated a potential of IPAA with short-time irradiation for the geochemical (mainly major element) analysis. Although IPAA may not be suitable for the whole rock analysis in state-of-the-art academic petrology and mineralogy research due to, e.g., insufficient precision and difficulties in P determination, there are applications where IPAA could benefit over the common, standard non-radioanalytical methods. Such applications include rapid analysis of large series of samples when rapid rock characterization is more important than are the highest accuracy and precision, analysis of samples that are difficult to dissolve or to homogenize, nondestructive analysis of “mini-cores” taken from industrial or scientific drill-cores or from building materials (concrete, building stone), etc.

Application of the method should be interesting mainly for laboratories equipped with electron accelerators that already have experience with IPAA but probably utilize its long-time irradiation mode only. A similar situation may exist in many INAA laboratories that often perform long-time irradiation of INAA for trace element analysis but do not employ the short-lived activation products for major element analysis. The reasons for not applying the short-time irradiation mode, both for IPAA and INAA users, are often just technical limitations of their irradiation facilities, which are not equipped with a sufficiently fast sample transport system. The potential of the method, particularly for analysis of larger bulk samples, could attract IPAA newcomers or future users (e.g., experienced INAA users already equipped and licensed for radioactivity treatment and measurement), especially with increasing availability of clinical linacs suitable after modification for IPAA [20,21].

Author Contributions: Conceptualization, I.K., J.M. and Z.Ř.; methodology, Z.Ř., J.M., I.K. and D.C.; software, P.K.; validation, I.K. and J.M.; investigation, I.K. and D.C.; resources, J.M. and Z.Ř.; writing—original draft preparation, I.K. and J.M.; writing—review and editing, J.M.; supervision, J.M.; project administration, J.M.; funding acquisition, J.M. and Z.Ř. All authors have read and agreed to the published version of the manuscript.

Funding: This research was funded by the Czech Science Foundation, grants numbers 13 27885S and P108/12/G108.

Data Availability Statement: The data presented in tables are openly available in references stated with the tables or on request from the corresponding author.

Conflicts of Interest: The authors declare no conflict of interest.

References

1. Jackson, L.L.; Brown, F.W. Major and minor elements requiring individual determination, classical whole rock analysis, and rapid rock analysis. In *Methods for Geochemical Analysis (U.S. Geological Survey Bulletin 1770)*; Baedeker, P.A., Ed.; United States Government Printing Office: Denver, CO, USA, 1987; pp. G1–G23. [CrossRef]
2. Gill, R. (Ed.) *Modern Analytical Geochemistry: An Introduction to Quantitative Chemical Analysis Techniques for Earth, Environmental and Materials Scientists*; Longman Geochemistry Series; Routledge: New York, NY, USA, 1997; 34p, ISBN 978-0582099449.
3. The Elemental Analysis of Geological Materials: Elegant Solutions from SPECTRO Analytical Instruments (Rev.1). Available online: https://extranet.spectro.com/-/media/ametekspectroextranet/files/repeated/2013/the_elemental_analysis_of_geological_materials_r1_sep2013_web0.pdf?dmc=1&la=en (accessed on 2 April 2021).
4. Greenberg, R.R.; Bode, P.; De Nadai Fernandes, E.A. Neutron activation analysis: A primary method of measurement. *Spectrochim. Acta Part B At. Spectrosc.* **2011**, *66*, 193–241. [CrossRef]
5. Řanda, Z.; Kučera, J.; Mizera, J.; Frána, J. Comparison of the role of photon and neutron activation analyses for elemental characterization of geological, biological and environmental materials. *J. Radioanal. Nucl. Chem.* **2007**, *271*, 589–596. [CrossRef]
6. Baker, C.A. Gamma-activation analysis. *Analyst* **1967**, *92*, 601–610. [CrossRef]
7. Lutz, G.J. Photon activation analysis—A review. *Anal. Chem.* **1971**, *43*, 93–103. [CrossRef]
8. Segebade, C.; Berger, A. Photon Activation Analysis. In *Encyclopedia of Analytical Chemistry*; Meyers, R.A., Ed.; John Wiley & Sons Ltd.: Hoboken, NJ, USA, 2008. [CrossRef]
9. Segebade, C.; Starovoitova, V.N.; Borgwardt, T.; Wells, D. Principles, methodologies, and applications of photon activation analysis: A review. *J. Radioanal. Nucl. Chem.* **2017**, *312*, 443–459. [CrossRef]
10. Lindstrom, R.M. Prompt-gamma activation analysis. *J. Res. Natl. Inst. Stand. Technol.* **1993**, *98*, 127–133. [CrossRef] [PubMed]

11. Perry, D.L.; Firestone, R.B.; Molnár, G.L.; Révay, Z.; Kasztovszky, Z.; Gatti, R.C.; Wilde, P. Neutron-induced prompt gamma activation analysis (PGAA) of metals and nonmetals in ocean floor geothermal vent-generated samples. *J. Anal. At. Spect.* **2002**, *17*, 32–37. [[CrossRef](#)]
12. Görner, W.; Haase, O.; Ostermann, M.; Segebade, C. Instrumental analysis of phosphorus in organic material using high energy beta-counting after photoactivation (IPAA). *J. Radioanal. Nucl. Chem.* **2008**, *276*, 251–255. [[CrossRef](#)]
13. Řanda, Z.; Kreisinger, F. Tables of nuclear constants for gamma-activation analysis. *J. Radioanal. Chem.* **1983**, *77*, 279–495. [[CrossRef](#)]
14. IAEA. *Handbook on Photonuclear Data for Applications. Cross Sections and Spectra (IAEA-TECDOC 1178)*; International Atomic Energy Agency (IAEA): Vienna, Austria, 2000.
15. Řanda, Z.; Špaček, B.; Kuncíř, J.; Benada, J. *Nondestructive Gamma Activation Analysis of Mineral Materials*; Nuclear Information Centre: Prague, Czech Republic, 1981.
16. Krausová, I. Short-Lived Products of Photonuclear Reactions with a Microtron and Their Application to Photon Activation Analysis. Ph.D. Thesis, Czech Technical University, Prague, Czech Republic, 2015.
17. Krist, P.; Horák, Z.; Mizera, J.; Chvátil, D.; Vognar, M.; Řanda, Z. Innovations at the MT 25 microtron aimed at applications in photon activation analysis. *J. Radioanal. Nucl. Chem.* **2015**, *304*, 183–188. [[CrossRef](#)]
18. Řanda, Z.; Špaček, B.; Mizera, J. Express determination of gold in large mass samples of gold ores by photoexcitation reaction with 10 MeV bremsstrahlung. *J. Radioanal. Nucl. Chem.* **2007**, *271*, 603–606. [[CrossRef](#)]
19. Overwater, R.M.W.; Bode, P.; de Goeij, J.J.M. Gamma-ray spectroscopy of voluminous sources. Corrections for source geometry and self-attenuation. *Nucl. Instrum. Methods Phys. Res. A* **1993**, *A324*, 209–218. [[CrossRef](#)]
20. Eke, C.; Boztosun, I.; Segebade, C. Photon activation analysis of sand samples from Antalya in Turkey with a clinical electron linear accelerator. *Radiochim. Acta* **2019**, *107*, 149–156. [[CrossRef](#)]
21. Tserenpil, S.; Segebade, C.P.; Dapo, H.; Boztosun, I.; Vostokin, G.K.; Maslov, O.D.; Belov, A.G. Feasibility of using “Off-The-Shelf” clinical linac for soil multi-elemental instrumental photon activation analysis. *J. Radioanal. Nucl. Chem.* **2019**, *322*, 337–346. [[CrossRef](#)]